Progress In Electromagnetics Research, Vol. 121, 39–52, 2011

EVOLUTION AND COLLAPSE OF A LORENTZ BEAM IN KERR MEDIUM

R.-P. Chen[1, 2] and C. H. Raymond Ooi[2, *]

[1]School of Sciences, Zhejiang A & F University, Lin'an, Zhejiang Province 311300, China

[2]Department of Physics, University of Malaya, Kuala Lumpur 50603, Malaysia

Abstract—The effect of Kerr nonlinearity on a Lorentz beam is investigated by using the nonlinear Schrödinger (NLS) equation. Based on the variational method, the evolution of a Lorentz beam in a Kerr medium is demonstrated and the critical collapse powers of the Lorentz beam are derived. Numerical simulations of the propagation of a Lorentz beam in a Kerr medium show that the beam becomes quasi-circular in a very short distance. Although the beam width of the Lorentz beam broadens, the central part of the beam give rise to a partial collapse.

1. INTRODUCTION

Recently, there has been growing interest in the Lorentz beam since it was introduced by Gawhary and Severini [1]. The beam is appropriate for describing certain laser sources, e.g., in double-heterojunction $Ga_{1-x}Al_xAs$ lasers [2, 3]. Recent investigations confirmed the importance of beam propagation properties in linear region [1–5]. The radiation force of highly focused Lorentz-Gauss beams on a dielectric sphere has been studied in the Rayleigh scattering regime [6]. An interesting aspect of beam propagation in nonlinear medium is the emergence of solitons, recently being studied in optical fibers using Ginzburg-Landau equation [7], nonlinear microring and nanostructures [8], left-handed structures [9] and system with parabolic nonlinearity [10].

In this work, we study, analytically and numerically, the effect of Kerr nonlinearity on the Lorentz beam using nonlinear Schrödinger

Received 17 August 2011, Accepted 8 October 2011, Scheduled 13 October 2011

* Corresponding author: C. H. Raymond Ooi (rooi@um.edu.my).

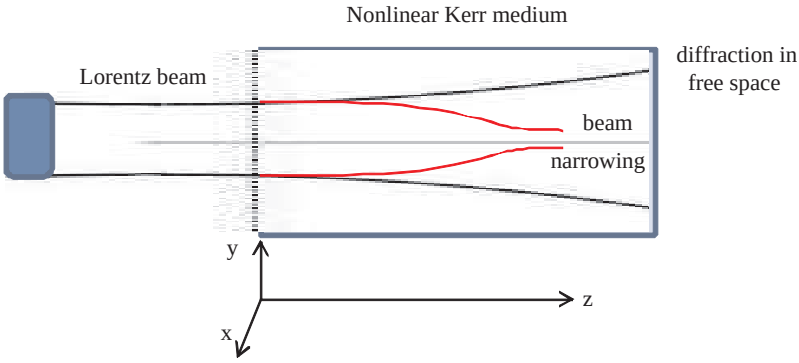

Figure 1. (Color online) Collapse and narrowing of a Lorentz beam width in a nonlinear Kerr medium. The beam would diverge in free space due to diffraction.

(NLS) equation, as depicted in Fig. 1. The Kerr medium has an intensity-dependent refractive index, $n = n_0 + n_2|E|^2$ that is due to third order nonlinear response of the polarization to electric field of the beam or laser light. Recent works have studied the propagation of elliptic Gaussian beam [11] and beams with unequal transverse widths [12] in Kerr medium, as well as soliton propagation in Kerr [13] and non-Kerr law media [14]. We compute the spatial distribution of the Lorentz beam as it propagates through the nonlinear Kerr medium, including the critical power and collapse. It is important for understanding the effects of beam divergence due to diffraction and focusing due to the Kerr nonlinearity on the propagation and spatial distribution of the Lorentz beam.

This work is beneficial for various applications in optics. The study of Lorentz beam propagation and focusing can be extended to novel chiral waveguides [15, 16], optical fiber filled with liquid crystals [17], turbulent environment [18] as well as medium with exotic electrodynamics [19]. Further analysis on scattering of the Lorentz beam by metallic spheres [20] and negative refractive index materials [21] would be useful for developing plasmonic devices with subwavelength optical resolution.

The propagation of pulses in nonlinear Kerr medium has been studied using various methods, including nonstationary time domain techniques involving the Green's function [22], multiple scale analysis [23] and quasi-particle theory for colliding solitons [24]. Variational technique has been applied to waveguides with effective refractive index method [25] and the study of optical solitons with higher order dispersions [26].

We apply the variational approach [27–31] to obtain important information about the nonlinear dynamics on the spatial distributions of the Lorentz beam in the Kerr medium. We obtain the critical power [32–42] of the Lorentz beam with uniform wavefront, which is required to collapse the beams, as a function of different beam parameters, particularly the waists w_{0x} and w_{0y}. Numerical simulations illustrate in more details the nonlinear dynamics of the beams in the Kerr medium. The simulations of the propagation of the Lorentz beam in Kerr media show that the symmetrical Lorentz beam ($w_{0y} = w_{0x}$) becomes quasi-circular in a very short distance z. For an asymmetrical Lorentz beam, the central part of the beam also become quasi-circular in a certain distance. Although the beam width of the Lorentz beam broadens as predicted by the variational approach, the central part of the beams give rise to radial compression during propagation in Kerr medium, the beams will give rise to a partial collapse when the input power reaches a certain threshold below the critical power.

2. PROPAGATION OF A LORENTZ BEAM IN A KERR MEDIUM

The propagation of a light beam in a Kerr medium, under the paraxial approximation, can be described by the NLS equation:

$$\left(\frac{\partial^2}{\partial x^2} + \frac{\partial^2}{\partial y^2} - 2ik\frac{\partial}{\partial z}\right) E + 2k^2\frac{n_2}{n_0}\left|E\right|^2 E = 0, \tag{1}$$

where k is the linear wavevector, x and y are the transverse coordinates, z is the longitudinal coordinate, n_2 is the third order nonlinear coefficient and n_0 is the linear refractive index of the medium.

We can reformulate Eq. (1) as a variational problem [27–29] using the appropriate Lagrangian,

$$L = \left|\frac{\partial E}{\partial x}\right|^2 + \left|\frac{\partial E}{\partial y}\right|^2 - ik\left(E\frac{\partial E^*}{\partial z} - E^*\frac{\partial E}{\partial z}\right) - \frac{n_2 k^2}{n_0}\left|E\right|^4. \tag{2}$$

where * indicates the complex conjugation. We use the Lorentz field distribution as a trial solution for the procedure of the variational approach:

$$E\left(x, y, z\right) = \frac{A(z)\exp\left[i\theta(z) + iS_1(z)x^2 + iS_2(z)y^2\right]}{w_x w_y\left[1 + (x/w_x)^2\right]\left[1 + (y/w_y)^2\right]}, \tag{3}$$

where $A(z)$ and $\theta(z)$ are the amplitude and phase of the complex amplitude $E(x, y, z)$, w_x and w_y are the parameters which are associated to beam widths of a Lorentz beam in the x- and y-directions,

respectively. $S_1(z)$ and $S_2(z)$ are the beam normalized inverse of curvature. Note that a quadratic phase approximation (QPA) [30–34] has been introduced here. Substitution of the trial function Eq. (3) into Eq. (2), and integration with respect to x and y yield $\langle L\rangle = \int L dxdy$ the effective Lagrangian

$$\begin{aligned}\langle L\rangle \;=\; & \frac{\pi^2 A(z)^2}{w_x w_y}\left[\frac{1}{8}\left(\frac{1}{w_x^2}+\frac{1}{w_y^2}\right)+S_1(z)^2 w_x^2+S_2(z)^2 w_y^2\right.\\ & \left.+\frac{k}{2}\left(\frac{\partial\theta(z)}{\partial z}+w_x^2\frac{\partial S_1(z)}{\partial z}+w_y^2\frac{\partial S_2(z)}{\partial z}\right)\right]\\ & -\frac{25\pi^2 n_2 k^2 A(z)^4}{256 n_0 w_x^3 w_y^3}.\end{aligned} \tag{4}$$

From the reduced variational principle, $\delta\int\langle L\rangle\, dz = 0$ and Eq. (4), we obtain a set of coupled ordinary differential equations that describes the evolution of the Lorentz beam in the Kerr medium:

$$\frac{A(z)^2}{w_x w_y} \;=\; \frac{A(z=0)^2}{w_{0x} w_{0y}}, \tag{5}$$

$$S_1(z) \;=\; \frac{k}{2w_x}\frac{dw_x}{dz}, \qquad S_2(z)=\frac{k}{2w_y}\frac{dw_y}{dz}, \tag{6}$$

$$\frac{d^2 w_x}{dz^2} \;=\; \frac{1}{2k^2 w_x^3}\left(1-\beta\frac{w_x}{w_y}\right), \tag{7}$$

$$\frac{d^2 w_y}{dz^2} \;=\; \frac{1}{2k^2 w_y^3}\left(1-\beta\frac{w_y}{w_x}\right), \tag{8}$$

where $\beta = \frac{25A(z)^2 n_2 k^2}{64 n_0 w_x w_y} = \frac{25A_0^2 n_2 k^2}{64 n_0 w_{0x} w_{0y}}$. The w_{0x} and w_{0y} are the parameters w_x and w_y at the waist plane ($z=0$).

The above equations are supplemented by an equation for phase,

$$\begin{aligned}\frac{\partial\theta(z)}{\partial z} =& \frac{25kn_2A(z)^2}{64n_0w_x^2w_y^2}-\frac{1}{4k}\left(\frac{1}{w_x^2}+\frac{1}{w_y^2}\right)\\ & -\frac{2S_1(z)^2w_x^2}{k}-\frac{2S_2(z)^2w_y^2}{k}\\ & -w_x^2\frac{\partial S_1(z)}{\partial z}-w_y^2\frac{\partial S_2(z)}{\partial z}.\end{aligned} \tag{9}$$

Eq. (5) implies the conservation of energy of the Lorentz beam. Eq. (6) shows transverse phase variation is generated by its deformation (change of the beam width). Eqs. (7) and (8) describe the evolutions of the beam widths of the Lorentz beam in the x- and y-directions,

respectively. The equations can be solved analytically to obtain

$$\begin{aligned} w^2(z) &= w_x^2 + w_y^2 \\ &= \frac{z^2}{2k^2}\left(\frac{1}{w_{0x}^2} + \frac{1}{w_{0y}^2} - \frac{2\beta}{w_{0x}w_{0y}}\right) \\ &\quad + w_{0x}^2\left(1 + \frac{2S_1(0)z}{k}\right)^2 + w_{0y}^2\left(1 + \frac{2S_2(0)z}{k}\right)^2. \end{aligned} \quad (10)$$

where $S_1(0)$ and $S_2(0)$ are not zero except for uniform wavefront. Eq. (10) describes the variation of the average width of the Lorentz beam in a Kerr medium. If the field is weak (small β) the width increases with z. For sufficiently strong field, such that $\beta > \frac{1}{2}(\frac{w_{0y}}{w_{0x}} + \frac{w_{0x}}{w_{0y}})$, self-focusing reduces the average width.

The critical power $P_{cr} = \iint_s |E_{cr}(x,y)|^2\, dxdy$ of the Lorentz beam which is required to collapse the beam to a uniform wavefront [32–34], i.e., $S_1(z=0) = 0$ and $S_2(z=0) = 0$, can be found by setting the width of the Lorentz beam invariant over z, i.e., $\beta = \frac{1}{2}(\frac{w_{0y}}{w_{0x}} + \frac{w_{0x}}{w_{0y}}) = \frac{25A(z)^2 n_2 k^2}{64 n_0 w_x w_y} = \frac{25A(z=0)^2 n_2 k^2}{64 n_0 w_{0x} w_{0y}}$. This gives

$$E_{cr}^2(x,y) = \frac{32n_0}{25n_2} \frac{\frac{1}{k^2 w_{0x} w_{0y}}\left(\frac{w_{0y}}{w_{0x}} + \frac{w_{0x}}{w_{0y}}\right)}{\left[1 + (\frac{x}{w_{0x}})^2\right]^2 \left[1 + (\frac{y}{w_{0y}})^2\right]^2} \quad (11)$$

$$P_{cr} = \frac{8\pi^2 n_0}{25 n_2 k^2}\left(\mu + \mu^{-1}\right) \quad (12)$$

where $\mu = w_{0y}/w_{0x}$ represents the asymmetry of the Lorentz beam. Eq. (12) implies that the critical collapse power of a Lorentz beam depends on the beam profile of the transverse distribution w_{0x}, w_{0y} and the nonlinear parameter n_2 of the medium. The power increases with the increasing asymmetry. When $w_{0x} = w_{0y}$, the critical collapse power is minimum $P_{cr}^{\min} = \frac{16\pi^2 n_0}{25 n_2 k^2}$, corresponding to a symmetrical Lorentz beam. The critical collapse power of a symmetrical Lorentz beam only depends on the nonlinear parameter of the medium, and is almost equal to that of the Gaussian beam $P_{cr}^{GS} = \frac{2\pi n_0}{n_2 k^2}$ [38–42]. The ratio of the critical power of a symmetrical Lorentz beam to that of a Gaussian beam is $8\pi/25$. Obviously, the critical collapse power described by Eq. (12) is the upper bound for Lorentz beam. The critical power overestimates the actual threshold power for collapse [35–42].

If only diffraction effect and the self-focusing due to the Kerr effect are considered, the theoretical analysis indicates that when the initial

power exceeds the critical power, the beam width goes to zero in a finite propagation distance. Since $P_{in} = \frac{1}{4}\frac{\pi^2 A(z)^2}{w_x w_y}$, the bracket term in the first line of Eq. (10) is $\frac{16\pi n_0}{25 n_2 k^2 w_{0x} w_{0y}}(P_{cr} - P_{in})$. So, the variational approach predicts that when $P_{in} > P_{cr}$ the beam width of a Lorentz beam goes to zero in a finite propagation distance. Although this is unrealistic, the approach provides a qualitative picture. In fact, when the initial power becomes too high, other nonlinear effects that give modulation instability like higher order nonlinearity, self steepening and self-phase modulation should be considered, and higher-order processes such as plasma generation halt the collapse [42]. Also, for ultrashort laser pulse, the numerical calculation of the NLS in the Kerr medium must go beyond the paraxial approximation.

3. NUMERICAL RESULTS AND DISCUSSION

In order to investigate further the effect of Kerr nonlinearity [23–36] on the Lorentz beam, we need to solve the NLS equation numerically. Numerical simulations were done using the parameters of wavelength $\lambda = 0.53\,\mu\text{m}$, $n_0 = 1$, $n_2 = 0.5 \times 10^{-4}\,\text{cm}^2/\text{GW}$, $w_{0x} = 10\,\mu\text{m}$ and $z_0 = kw_{0x}^2/2 = 0.6\,\text{mm}$, respectively. As demonstrated above, the variational approach has shown that a non-diffracting situation is possible to obtain by balancing linear diffraction and nonlinear focusing. When the initial power exceeds the critical power, the beam width goes to zero in a finite propagation distance, a global collapse occurs. By using numerical simulations with the Lorentz beam for varying degrees of incident powers, the peak intensity as a function

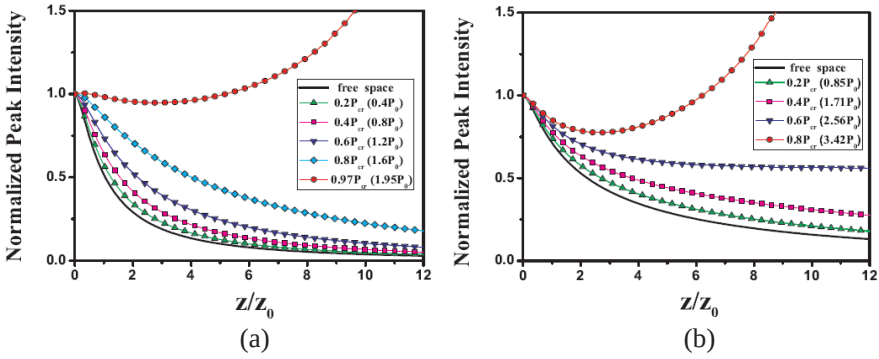

Figure 2. (Color online) The peak intensity of Lorentz beam as a function of the propagation distance with different initial powers. Numerical results for (a) $w_{0y} = w_{0x}$; (b) $4w_{0y} = w_{0x}$.

of the propagation distance with different initial powers are shown in Fig. 2 for the cases: (a) $w_{0x} = w_{0y}$; (b) $w_{0x} = 4w_{0y}$. The figures have been normalized to their initial peak intensities. For the sake of intuition, the initial powers have been specified not only in terms of P_{cr}, but also in terms of $P_0 = \pi n_0/(n_2 k^2)$. The simulations show that as the initial power reaches a certain threshold, the intensity at the center part of the beam will dominate [35–42] and the peak intensity increases with distance z. This threshold is lower for asymmetric beam (see Fig. 2). It indicates that when the initial power reach a certain threshold but is less than the critical power, the central part of the beam undergoes compression and gives rise to a partial collapse. The phenomena have be studied extensively, for example, by Fibich and Ilan [41]. Fig. 2 shows the results of numerical computation. By comparing the numerical simulation results and the analytical predictions by the variational approach, also as shown in Figs. 3 and 4 asymmetric, it is found that when the initial power is high and comparable to the critical power, there is a substantial discrepancy between the analytical predictions by the variational method and the numerical simulation results. It can be explained as the analytical predictions is based on the trial solution Eq. (3), but the actual evolution of the Lorentz beam in Kerr medium is difficult to be described by an analytical expression, especially in the region of collapse. Under the condition that the

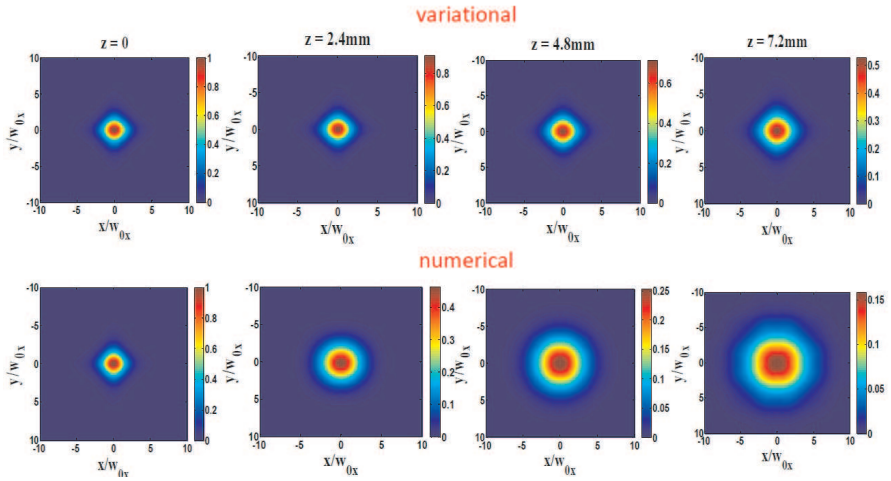

Figure 3. (Color online) Contour maps of the power distributions of the Lorentz beam with $w_{0x} = w_{0y}$ at several propagation distances with initial power $P_{in} = 0.8P_{cr} = 1.6P_0$ where $P_0 = \pi n_0/(n_2 k^2)$. The maximum scale (red) in the colorcode corresponds to the power P_{in}.

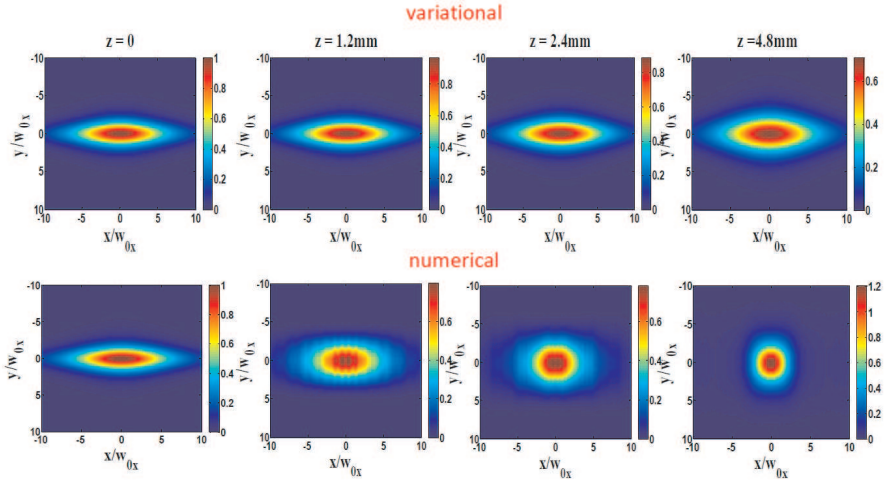

Figure 4. (Color online) The contour maps for the power distributions of the asymmetric Lorentz beam with $w_{0x} = 4w_{0y}$ and initial power $P_{in} = 0.8P_{cr} = 3.43P_0$.

initial power is much lower than the critical power, the evolution of the Lorentz beam in Kerr media can be approximately described by the trial solution Eq. (3), then the analytical predictions would agree well with the actual numerical results. Numerical calculations show that the critical power of a symmetrical Lorentz beam is $P_{cr}^{Ls} = 1.95\pi n_0/(n_2k^2)$ which is less than that predicted by the variational approach in Eq. (12), but slightly more than that of a Gaussian beam $P_{cr}^{G} = 1.89\pi n_0/(n_2k^2)$ as demonstrated by Fibich et al. in [41, 42].

We also consider the critical power of asymmetrical Lorentz beam. The collapse dynamics of elliptical beams have been extensively studied [22, 24]. These studies pointed out significant differences between quantitative predictions of the aberrationless approximation and actual results obtained from NLS equation simulations [24–41]. From our numerical calculations, we find a simple empirical expression for the critical power of asymmetrical Lorentz beam by fitting the results of the numerical calculation

$$P_{\rm cr}(\mu) = 1.95\,[0.64 + 0.18\,(\mu{+}1/\mu)]\,\frac{\pi n_0}{n_2k^2}. \qquad (13)$$

This empirical formula is in agreement with exact numerical results within 1.5% for $1/4 < \mu < 4$. The impact of asymmetry on the critical power of a Lorentz beam is less than the ellipticity on a Gaussian beam as demonstrated in [41, 42]. This phenomenon can be explained as the particular profile of the Lorentz beam that is bell-shaped curve and

long tail, and noncircular symmetrical. With the spatial extension being the same, the angular spreading of a Lorentz distribution is higher than that of a Gaussian description.

The contour plots of the intensity distributions as a function of the propagation distance are shown in Figs. 3 and 4 with different initial widths: $w_{0x} = w_{0y}$ and $w_{0x} = 4w_{0y}$. Again, the plots have been normalized to their initial peak intensities. Careful analysis of the simulation of the propagation of the Lorentz beam in the Kerr media shows that a symmetrical Lorentz beam ($w_{0x} = w_{0y}$) becomes quasi-circular in a very short distance as shown in Fig. 3.

For a asymmetrical Lorentz beam, the numerical simulations

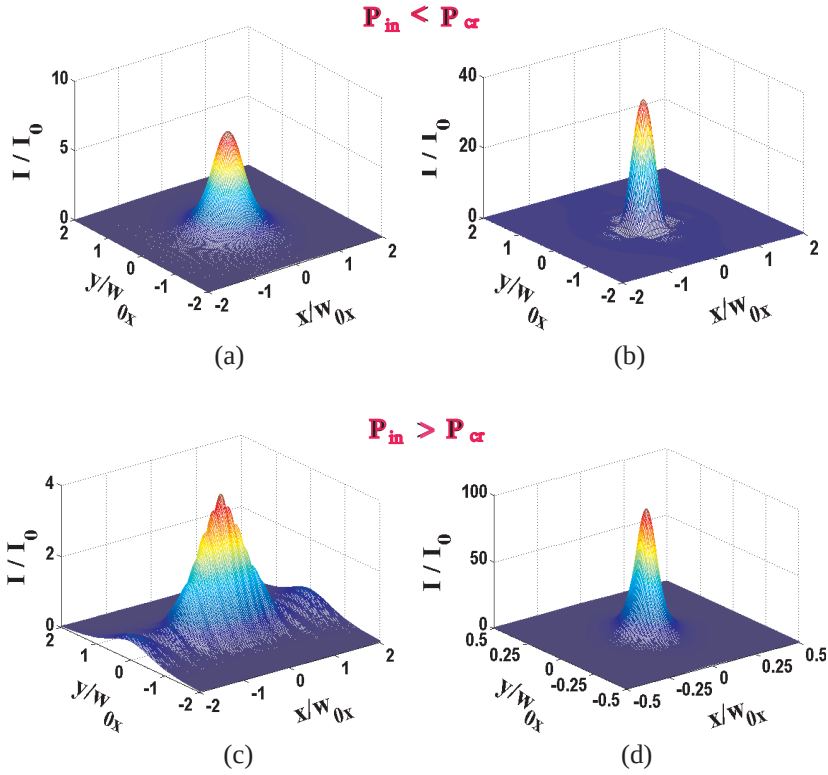

Figure 5. (Color online) The intensity distributions obtained from numerical solutions of NLS equation showing narrowing of the asymmetric Lorentz beam with $w_{0x} = 4w_{0y}$ and initial power $P_{in} = 0.8P_{cr} = 3.43P_0$ at propagation distances. (a) $z = 12z_0$. (b) $z = 13z_0$, and with initial power $P_{in} = 1.8P_{cr} = 7.72P_0$ in propagation distances. (c) $z = 2.5z_0$. (d) $z = 3z_0$. Note that the scale in (d) is about five times smaller.

indicate that when the beam undergoes moderate focusing, the central part of the beam becomes quasi-circular at a certain distance, changing from elliptic to a circular Townes profile, as shown in Fig. 4. This is somewhat similar to that of the elliptic Gaussian beam [41]. As the propagation length increases, the high intensity (central) part of the beam is compressed to a smaller size (as can be seen from the right panel of Fig. 4) and eventually leads to the collapse. Numerical calculations show that the partial collapse occurs at the propagation distance $z = 14z_0$ in the asymmetric case, i.e., $w_{0x} = 4w_{0y}$ with $P_{in} = 0.8P_{cr} = 3.43P_0$.

Figures 5(a) and (b) show the results of the intensity distribution at propagation distances $z = 12z_0$ and $z = 13z_0$ when the initial power reaches a certain threshold power which is below the critical power for a global collapse predicted by variational method. When $P_{in} > P_{cr}$, the beam collapses at a much shorter propagation length, as shown in Figs. 5(c) and (d).

4. CONCLUSION

The propagation of a Lorentz beam in a Kerr medium has been studied by using the NLS equation. The evolution of the beam parameters is analyzed by variational approach. The critical power of the Lorentz beam with a uniform wavefront is derived. By using numerical simulations, the dynamic interaction between nonlinear focusing and linear diffraction has been demonstrated. Numerical simulations of the propagations of the asymmetric Lorentz beam in a Kerr medium show that the beams become quasi-circular within a very short distance. Although the beam width increases as predicted by the variational method when the incident power is smaller than the critical power, the partial collapse can still occur at the center parts of the Lorentz beam. At low intensity, the variational results can approximately predict the numerical results. However, when the input power and the asymmetry of a Lorentz beam are increased, the variational results significantly deviate from the numerical results.

ACKNOWLEDGMENT

This work is partially supported by the State Key Program for Basic Research of China under Grant No.2006CB921805, the Key Project of the Education Commission of Zhejiang Province of China and the University of Malaya (UM)/Ministry of Higher Education (MOHE) High Impact Research (HIR) programme Grant No. A-000004-50001.

REFERENCES

1. Gawhary, O. E. and S. Severini, "Lorentz beams and symmetry properties in paraxial optics," *J. Opt. A, Pure Appl. Opt.*, Vol. 8, 409–414, 2006.
2. Naqwi, A. and F. Durst, "Focusing of diode laser beams: A simple mathematical model," *Appl. Opt.*, Vol. 29, 1780–1785, 1990.
3. Dumke, W. P., "The angular beam divergence in double-heterojunction lasers with very thin active regions," *J. Quantum Electron.*, Vol. 11, 400–402, 1975.
4. Zhou, G., "Nonparaxial propagation of a Lorentz-Gauss beam," *J. Opt. Soc. Am. A*, Vol. 25, 2594–2599, 2008.
5. Zhou, G., "Propagation of a partially coherent Lorentz-Gauss beam through a paraxial ABCD optical system," *Opt. Express*, Vol. 18, 4637–4643, 2010.
6. Jiang, Y., K. Huang, and X. Lu, "Radiation force of highly focused Lorentz-Gauss beams on a Rayleigh particle," *Opt. Express*, Vol. 19, 9708–9713, 2011.
7. Biswas, A., "Temporal-soliton solution of the complex Ginzburg-Landau equation with power law nonlinearity," *Progress In Electromagnetics Research*, Vol. 96, 1–7, 2009.
8. Mitatha, S., "Dark soliton behaviors within the nonlinear micro and nanoring resonators and applications," *Progress In Electromagnetics Research*, Vol. 99, 383–404, 2009.
9. Gharakhili, F. G., M. Shahabadi, and M. Hakkak, "Bright and dark soliton generation in a left-handed nonlinear transmission line with series nonlinear capacitors," *Progress In Electromagnetics Research*, Vol. 96, 237–249, 2009.
10. Khalique, C. M. and A. Biswas, "Optical solitons with parabolic and dual-power nonlinearity via lie symmetry analysis," *Journal of Electromagnetic Waves and Applications*, Vol. 23, No. 7, 963–973, 2009.
11. Gross, B. and J. T. Manassah, "Numerical solution for the propagation of elliptic Gaussian beam in a Kerr medium," *Phys. Lett. A*, Vol. 169, 371–378, 1992.
12. Barthelemy, A., C. Froehly, S. Maneuf, and E Reynaud, "Experimental observation of beams' self-deflection appearing with two-dimensional spatial soliton propagation in bulk Kerr material," *Opt. Lett.*, Vol. 17, 844–846, 1992.
13. Crosignani, B. and P. D. Porto, "Nonlinear propagation in Kerr media of beams with unequal transverse widths," *Opt. Lett.*,

Vol. 18, 1394–1396, 1993.

14. Biswas, A., R. Kohl, M. E. Edwards, and E. Zerrad, "Soliton parameter dynamics in a non-Kerr law media," *Progress In Electromagnetics Research C*, Vol. 1, 1–35, 2008.
15. Xu, J., W.-X. Wang, L.-N. Yue, Y.-B. Gong, Y.-Y. Wei, "Electromagnetic wave propagation in an elliptical chiroferrite waveguide," *Journal of Electromagnetic Waves and Applications*, Vol. 23, No. 14–15, 2021–2030, 2009.
16. Topa, A. L., C. R. Paiva, and A. M. Barbosa, "Electromagnetic wave propagation in chiral H-guides," *Progress In Electromagnetics Research*, Vol. 103, 285–303, 2010.
17. Choudhury, P. K. and W. K. Soon, "TE mode propagation through tapered core liquid crystal optical fibers," *Progress In Electromagnetics Research*, Vol. 104, 449–463, 2010.
18. Wei, H.-Y., Z.-S. Wu, and Q. Ma, "Log-amplitude variance of laser beam propagation on the slant path through the turbulent atmosphere," *Progress In Electromagnetics Research*, Vol. 108, 277–291, 2010.
19. Costa-Quintana, J. and F. Lopez-Aguilar, "Propagation of electromagnetic waves in material media with magnetic monopoles," *Progress In Electromagnetics Research*, Vol. 110, 267–295, 2010.
20. Apostol, M. and G. Vaman, "Plasmons and diffraction of an electromagnetic plane wave by a metallic sphere," *Progress In Electromagnetics Research*, Vol. 98, 97–118, 2009.
21. Cao, P., X. Zhang, L. Cheng, and Q. Meng, "Far field imaging research based on multilayer positive- and negative-refractive-index media under off-axis illumination," *Progress In Electromagnetics Research*, Vol. 98, 283–298, 2009.
22. Aberg, I., "High-frequency switching and Kerr effect-nonliear problems solved with nonstationary time domain techniques," *Progress In Electromagnetics Research*, Vol. 17, 185–235, 1997.
23. Zamani, A. K. and M. Shahabadi, "Multiple-scale analysis of plane wave refraction at a dielectric slab with Kerr-type nonlinearity," *Progress In Electromagnetics Research*, Vol. 56, 81–92, 2006.
24. Konar, S. and A. Biswas, "Intra-channel collision of Kerr law optical solitons," *Progress In Electromagnetics Research*, Vol. 53, 55–67, 2005.
25. Benson, T. M. and P. C. Kendall, "Variational techniques including effective and weighted index methods," *Progress In Electromagnetics Research*, Vol. 10, 1–40, 1995.

26. Green, P. D., D. Milovic, D. A. Lott, and A. Biswas, "Optical solitons with higher order dispersion by semi-inverse variational principle," *Progress In Electromagnetics Research*, Vol. 102, 337–350, 2010.
27. Anderson, D. and M. Bonnedal, "Variational approach to nonlinear self-focusing of Gaussian laser beams," *Phys. Fluids*, Vol. 22, 105–109, 1979.
28. Anderson, D., "Variational approach to nonlinear pulse propagation in optical fibers," *Phys. Rev. A*, Vol. 27, 3135–3145, 1983.
29. Malomed, B., "Variational methods in nonlinear fiber optics and related fields," *Prog. Opt.*, Vol. 43, 70–191, 2002.
30. Pérez-Garćia, V. M., P. Torres, and G. D. Montesinos, "The method of moments for nonlinear Schrödinger equations: Theory and applications," *SIAM J. Appl. Math.*, Vol. 67, 990–1015, 2007.
31. Pérez-Garćia, V. M., "Self-similar solutions and collective coordinate methods for nonlinear Schrödinger equations," *Phys. D*, Vol. 191, 211–218, 2004.
32. Vlasov, S. N., V. A. Petrishchev, and V. I. Talanov, "Averaged description of wave beams in linear and nonlinear media (the method of moments)," *Radio. Quan. Electron.*, Vol. 14, 1062–1070, 1971.
33. Fibich, G. and G. Papanicolau, "Self-focusing in the perturbed and unperturbed nonlinear Schrödinger equation in critical dimension," *SIAM J. Appl. Math.*, Vol. 60, 183–240, 1999.
34. Vlasov, S. N., S. N. Gurbatov, and L. V. Piskunov, "Self-focusing of wave beams having an elliptical cross section," *Radiofizika*, Vol. 17, 1805–1811, 1974.
35. Johannisson, P., D. Anderson, M. Lisak, and M. Marklund, "Nonlinear Bessel beams," *Opt. Commun.*, Vol. 222, 107–115, 2003.
36. Chen, R. P., C. F. Yin, X. X. Chu, and H. Wang, "Effect of kerr nonlinearity on an Airy beam," *Phys. Rev. A*, Vol. 82, 043832, 2010.
37. Chen, R. P., Y. Z. Ni, and X. X. Chu, "Propagation of a cos-Gaussian beam in a kerr medium," *Opt. Laser Tech.*, Vol. 43, 483–487, 2011.
38. Grow, T. D., A. A. Ishaaya, L. T. Vuong, A. L. Gaeta, N. Gavish, and G. Fibich, "Collapse dynamics of super-Gaussian beams," *Opt. Express*, Vol. 14, 5468–5475, 2006.
39. Moll, K. D., A. L. Gaeta, and G. Fibich, "Self-similar optical wave collapse: Observation of the Townes profile," *Phys. Rew.*

Lett., Vol. 90, 203902, 2003.

40. Feit, M. D. and J. A. Fleck, "Beam nonparaxiality, filament formation, and beam breakup in the self-focusing of optical beams," *J. Opt. Soc. Am. B*, Vol. 5, 633–640, 1988.
41. Fibich, G. and B. Ilan, "Self-focusing of elliptic beams: An example of the failure of the aberrationless approximation," *J. Opt. Soc. Am. B*, Vol. 17, 1749–1758, 2000.
42. Fibich, G. and A. L. Gaeta, "Critical power for self-focusing in bulk media and in hollow waveguides," *Opt. Lett.*, Vol. 25, 335–337, 2000.